

Superstructure of hollandite $K_xMg_{(8+x)/3}Sb_{(16-x)/3}O_{16}$ ($x \approx 1.76$)

Yuichi Michiue*

National Institute for Materials Science, 1-1 Namiki, Tsukuba, Ibaraki 305-0044, Japan

Received 19 February 2007; received in revised form 6 April 2007; accepted 10 April 2007

Available online 19 April 2007

Abstract

Single crystals of $K_xMg_{(8+x)/3}Sb_{(16-x)/3}O_{16}$ ($x \approx 1.76$) with a hollandite superstructure were grown. Ordering schemes for guest ions (K) and the host structure were confirmed by the structure refinement using X-ray diffraction intensities. The space group is $I4/m$ and cell parameters are $a = 10.3256(6)$, $c = 9.2526(17)\text{\AA}$ with $Z = 3$. Superlattice formation is primarily attributed to the Mg/Sb occupational modulation in the host structure. Mg/Sb ratios at two nonequivalent metal sites are 0.8977/0.1023 and 0.1612/0.8388. Two types of the cavity are seen in the tunnel, where parts of K ions deviate from the cavity center along the tunnel direction. Probability densities for K ions in the two cavities are different from each other, which seems to have arisen from the Mg/Sb modulation.

© 2007 Elsevier Inc. All rights reserved.

Keywords: Hollandite; Superstructure; Occupational modulation; X-ray diffraction

1. Introduction

The one-dimensional (1d) tunnel in hollandite structures is used as a container for radioactive wastes [1], or an ionic conduction path [2,3]. In addition, hollandite structures are of interest from a viewpoint of crystal chemistry, because diffraction patterns of some phases include (i) diffuse scattering in sheets normal to the tunnel direction, or (ii) commensurate or incommensurate satellite reflections. The first is due to short-range ordering of guest ions limited in a tunnel, while the second means 3d ordering of guest ions in tunnels and/or metal ions in the host structure. Diffuse scattering in K-hollandite, which was principally interpreted by assuming strong cation–cation interactions in a tunnel and no inter-tunnel correlations [4], was reproduced by a Frenkel–Kontorova model [5], a double chain model [6], and atomistic simulations by molecular dynamics method [7]. The 3d ordering is reported in many Ba-hollandites [8–11]. These structures can be considered as composite crystals constructed by two substructures; one is the host structure and another consists of guest ions. On the other hand, an incommensurate hollandite structure of

$La_xMo_8O_{16}$ was refined as not a composite crystal but a single modulated structure [12].

Chemical composition of hollandite in the system K_2O – MgO – Sb_2O_5 is generally given by $K_xMg_{(8+x)/3}Sb_{(16-x)/3}O_{16}$. Satellite reflections were observed at $c^*/3$ levels in rotation photographs for a single crystal of a phase with $x = \frac{4}{3}$, $K_{1.33}Mg_{3.11}Sb_{4.89}O_{16}$ [13], implying the formation for the superlattice of three times the sublattice along the tunnel direction. It was suggested by the computer simulation for electron diffraction patterns of the polycrystalline sample that the superlattice formation is due to the ordering of K ions in tunnels rather than the Mg/Sb ordering in the host structure [14]. However, no structure refinement has been reported for hollandite in which K ions are ordered in 3d manner. In this study, single crystals of $K_xMg_{(8+x)/3}Sb_{(16-x)/3}O_{16}$ ($x \approx 1.76$) with a hollandite superlattice were grown and the structure refinement has been carried out using X-ray diffraction intensities. Ordering schemes for guest ions and the host structure confirmed by the present study were different from those speculated for $K_{1.33}Mg_{3.11}Sb_{4.89}O_{16}$ in previous literature.

2. Experimental

Single crystals of hollandite were grown by the slow cooling method with excess alkali. A mixture of 0.184 g of

*Fax: +81 29 860 4662.

E-mail address: MICHIUE.Yuichi@nims.go.jp.

K_2CO_3 , 0.251 g of MgO , and 1.582 g of Sb_2O_5 ($\text{K}_2\text{CO}_3:\text{MgO}:\text{Sb}_2\text{O}_5 = 6:28:22$ in a molar ratio corresponding to $\text{K}_{4/3}\text{Mg}_{28/9}\text{Sb}_{44/9}\text{O}_{16}$) was heated with 0.055 g of K_2CO_3 ($\text{K}_{4/3}\text{Mg}_{28/9}\text{Sb}_{44/9}\text{O}_{16}:\text{K}_2\text{CO}_3 = 1:0.2$ in a molar ratio) at 1000°C for 30 min. A part of the sample was put in a sealed platinum tube, and heated at 1500°C for 150 min, then cooled to 1300°C at a rate of $-10^\circ\text{C}/\text{h}$, and taken out of the furnace. Along with polycrystalline products, plate (ilmenite $\text{Mg}_4\text{Sb}_2\text{O}_9$) and needle-shaped (hollandite) crystals were obtained. The composition parameter x in $\text{K}_x\text{Mg}_{(8+x)/3}\text{Sb}_{(16-x)/3}\text{O}_{16}$ for hollandite was estimated at 1.7–1.8 from EPMA measurements.

A single crystal of hollandite was mounted on a four-circle diffractometer. Conditions and parameters for data collection and refinement are listed in Table 1. At first, the structure was refined based on the superspace formalism for a commensurately modulated structure. The superspace group is $I4/m(00\gamma)$ [No. 12.1 in *International Tables for Crystallography* Vol. C (1999)] with $\gamma = \frac{2}{3}$, as reflections indexed by $ha^* + kb^* + lc^* + m\mathbf{q}$ ($\mathbf{q} = 2\mathbf{c}^*/3$) show the systematic condition of $h+k+l = 2n$ (n : integer) for $hklm$. Symmetry operations with the conventional basis are $(0, 0, 0, 0; \frac{1}{2}, \frac{1}{2}, \frac{1}{2}, 0) + x_1, x_2, x_3, x_4; -x_1, -x_2, x_3, x_4; -x_2, x_1, x_3, x_4; x_2, -x_1, x_3, x_4; -x_1, -x_2, -x_3, -x_4; x_1, x_2, -x_3, -x_4; x_2, -x_1, -x_3, -x_4; -x_2, x_1, -x_3, -x_4$. Laue class of

the superstructure indexed by $ha^* + kb^* + lc^*$ ($\mathbf{c}^* = \mathbf{c}^*/3$) is $4/m$, and systematic reflection conditions were $h+k+l = 2n$ (n : integer) for hkl , implying the space group of the highest symmetry $I4/m$ for the superstructure. From the superspace model two types of the superstructure with the space group $I4/m$ are possible, which are given by 3d sections at $t_0 = 0$ (model I) and $t_0 = \frac{1}{2}$ (model II). In both models a normal K-hollandite structure [15] was taken as a basic structure, and constraint conditions were imposed so that the charge neutrality is kept in a whole crystal. A program package *JANA2000* [16] was used for least-squares refinements and other calculations.

It was found that the reliability factors were markedly reduced by considering the modulation in occupation factors at the framework metal site in both models. Modulation functions for occupation factors of Sb and Mg ions in model I are given in Fig. 1, which are almost identical to those in model II. Reliability factors for model I ($R_{\text{obs}}(F) = 0.0210$ and $wR_{\text{obs}}(F^2) = 0.0423$) were a little larger than those for model II ($R_{\text{obs}}(F) = 0.0199$ and $wR_{\text{obs}}(F^2) = 0.0399$). In addition, the occupation factor of the Sb ion exceeded 1, and consequently that of the Mg ion was negative, at $t = 0$ in model I. (Note that occupation factors at framework metal sites in model I are given by values at $t = 0, \frac{1}{3}$, and $\frac{2}{3}$ in Fig. 1, while those in model II are given at $t = \frac{1}{6}, \frac{1}{2}$, and $\frac{5}{6}$.) The refinement for model I with the additional constraint condition was tried so that the occupation factor of the Sb at $t = 0$ was fixed to 1. However, the result became worse ($R_{\text{obs}}(F) = 0.0323$ and $wR_{\text{obs}}(F^2) = 0.0748$) and the total K content in a subcell exceeded 2, which is obviously impossible in the K-hollandite structure. Therefore, model I was discarded. Parameters for the superstructure obtained by the transformation of model II are given in Table 2. (Structural parameters of model II in superspace description are given as a Supplementary material.)

Table 1
Crystallographic data and conditions for data collection and refinement for $\text{K}_x\text{Mg}_{(8+x)/3}\text{Sb}_{(16-x)/3}\text{O}_{16}$ ($x \approx 1.76$)

M_r	981.7
Crystal system	Tetragonal
Space group	$I4/m$
a (Å)	10.3256(6)
c	9.2526(17)
V (Å ³)	986.5(2)
Z	3
D_x (g/cm ³)	4.956
$\mu(\text{MoK}\alpha)$ (mm ⁻¹)	10.44
Crystal size (mm)	0.05 × 0.05 × 0.40
Color	Transparent
Radiation	MoK α (0.71069 Å) (graphite-monochromatized)
Refinement of cell parameters	25 reflections ($40^\circ \leq 2\theta \leq 45^\circ$)
Scan mode	ω - 2θ
$2\theta_{\text{max}}$	100°
Range of h, k, l	$0 \leq h \leq 22, -22 \leq k \leq 22, -19 \leq l \leq 19$
Standard reflections	3 every 200
Reflections measured	10719
Independent reflections	2697
Observed reflections ($I_o > 3\sigma(I_o)$)	2097
R_{int}	0.0401
Absorption correction	Analytical
Transmission factor	0.198–0.627
Refinement on	F^2
$R_{\text{obs}}(F), wR_{\text{obs}}(F^2), S_{\text{obs}}$	0.0199, 0.0399, 1.32
$R_{\text{all}}(F), wR_{\text{all}}(F^2), S_{\text{all}}$	0.0340, 0.0438, 1.27
Weight factor	$1/[\sigma(I_o)^2 + 0.0001I_o^2]$
$\Delta\rho_{\text{min}} \Delta\rho_{\text{max}}$	-1.76 2.47(e/Å ³)

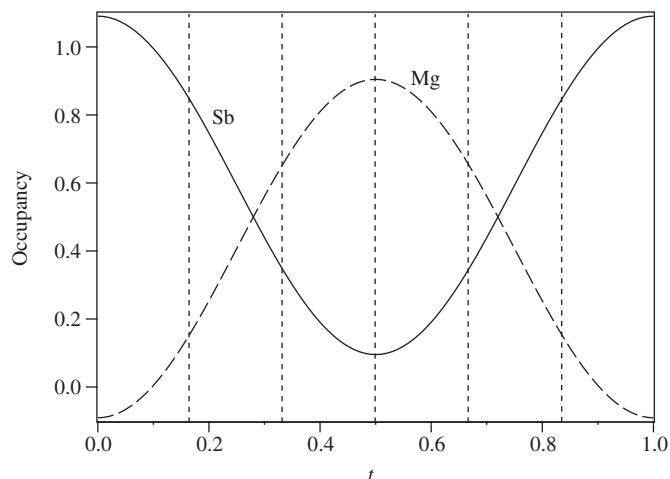


Fig. 1. Occupational modulation functions of metal ions in the host structure of $\text{K}_x\text{Mg}_{(8+x)/3}\text{Sb}_{(16-x)/3}\text{O}_{16}$ ($x \approx 1.76$).

Table 2

Occupancies, atomic coordinates, and thermal parameters of $K_xMg_{(8+x)/3}Sb_{(16-x)/3}O_{16}$ ($x \approx 1.76$)

Atom	Occupancy	<i>x</i>	<i>y</i>	<i>z</i>	U _{eq} (Å ²)	
K1	0.62(2)	0	0	0.1679(4)	0.057(3)	
K2	0.63(3)	0	0	0.5	0.074(3)	
K3	0.119(9)	0	0	0.0797(18)	0.034(3)	
K4	0.185(18)	0	0	0.426(3)	0.045(4)	
K5	0.08(4)	0	0	0.778(15)	0.07(3)	
M1 (Mg/Sb)	0.8977/0.1023(14)	0.35035(4)	0.16334(5)	0	0.00837(11)	
M2 (Mg/Sb)	0.1612/0.8388(11)	0.349673(7)	0.167161(7)	0.333197(7)	0.004944(17)	
O1	1	0.14859(14)	0.20550(13)	0	0.0095(2)	
O2	1	0.15617(9)	0.20079(9)	0.32768(11)	0.00888(16)	
O3	1	0.54488(12)	0.16350(15)	0	0.0094(2)	
O4	1	0.53960(8)	0.16434(10)	0.32692(10)	0.00902(16)	
Atom	U ¹¹	U ²²	U ³³	U ¹²	U ¹³	U ²³
K1	0.068(3)	= U ¹¹	0.036(2)	0	0	0
K2	0.090(4)	= U ¹¹	0.042(5)	0	0	0
K3	0.019(2)	= U ¹¹	0.064(9)	0	0	0
K4	0.032(3)	= U ¹¹	0.070(11)	0	0	0
K5	0.018(5)	= U ¹¹	0.18(8)	0	0	0
M1	0.00828(19)	0.00957(19)	0.00726(17)	0.00012(13)	0	0
M2	0.00502(3)	0.00535(3)	0.00446(3)	0.00037(2)	0.000095(19)	0.000106(19)
O1	0.0104(4)	0.0081(4)	0.0099(4)	−0.0002(3)	0	0
O2	0.0083(3)	0.0088(3)	0.0095(3)	−0.0004(2)	0.0010(2)	0.0008(2)
O3	0.0055(3)	0.0148(5)	0.0077(4)	0.0002(3)	0	0
O4	0.0054(2)	0.0140(3)	0.0076(3)	0.0004(2)	0.0001(2)	−0.0008(3)

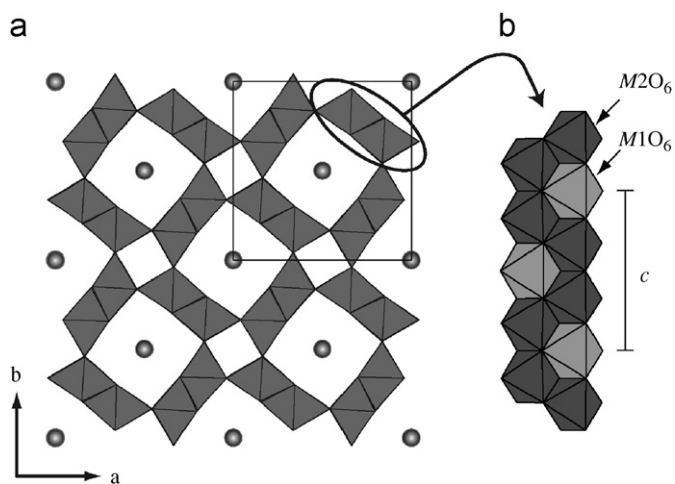


Fig. 2. Structure of $K_xMg_{(8+x)/3}Sb_{(16-x)/3}O_{16}$ ($x \approx 1.76$) projected along (a) the *c*-axis and (b) a direction normal to the *c*-axis. Lighter and darker shaded octahedra represent $M1O_6$ and $M2O_6$, respectively. Spheres are K ions.

3. Results and discussion

3.1. Host structure

In the host framework, zigzag ribbons consisting of edge-shared $M1O_6$ and $M2O_6$ octahedra extend along the *c*-axis (Fig. 2). Four ribbons around a 4-fold axis are connected by vertexes to form a tunnel. Interatomic distances between the metal site and oxygen ions forming coordination octahedra are listed in Table 3. The average

Table 3
Interatomic distances (Å) in $K_xMg_{(8+x)/3}Sb_{(16-x)/3}O_{16}$ ($x \approx 1.76$)

M1–O1	2.1283(15)	K1–O1 × 4	3.045(2)
M1–O2 × 2	2.1249(10)	K1–O2 × 4	3.014(2)
M1–O3	2.0086(13)		
M1–O4 × 2	2.0543(9)	K2–O2 × 8	3.0726(10)
Average	2.0826		
		K3–O1 × 4	2.720(5)
M2–O1	2.0276(8)	K3–O2 × 4	3.488(11)
M2–O2	2.0287(10)		
M2–O2	2.0195(10)	K4–O2 × 4	2.781(8)
M2–O3	1.9987(8)	K4–O2 × 4	3.474(16)
M2–O4	1.9622(9)		
M2–O4	1.9876(9)	K5–O1 × 4	3.33(9)
Average	2.0041	K5–O2 × 4	2.80(5)

distance for the $M1O_6$ octahedron is larger than that for the $M2O_6$, which is explained by the Mg/Sb occupation ratios at the two site, 0.8977/0.1023 at M1 and 0.1612/0.8388(11) at M2, and ionic radii 0.720 Å for Mg^{2+} and 0.60 Å for Sb^{5+} in six coordination [17].

The hollandite structure has two tunnels in a unit cell: one with the center axis (0, 0, *z*) and another with the center axis ($\frac{1}{2}, \frac{1}{2}, z$), which are equivalent because of the body-centered lattice. In order to avoid the confusion, the first tunnel with the center axis (0, 0, *z*) is taken for discussion hereafter. (The same discussion is applicable to the second tunnel considering the shift by $\frac{1}{2}$ in the fractional coordinate for *z*.) The tunnel in the hollandite structure is a linear

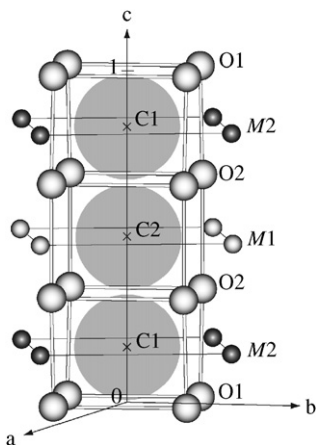


Fig. 3. Two types of the cavity in the tunnel of a supercell of $K_xMg_{(8+x)/3}Sb_{(16-x)/3}O_{16}$ ($x \approx 1.76$).

connection of pseudocuboctahedral cavities. There are two types of cavities in the tunnel of a supercell as shown in Fig. 3. One is around $(0, 0, \frac{1}{6})$ and $(0, 0, \frac{5}{6})$, and another is around $(0, 0, \frac{1}{2})$. Hereafter, the former cavity is called C1 and the latter is C2. As seen in Fig. 3, the nearest framework metals from the center of the cavity C1 are M2 sites, while those from the center of the C2 are M1. Composition-weighted mean of formal charges is 2.307 ($= 5 \times 0.1023 + 2 \times 0.8977$) for the M1 site and 4.516 ($= 5 \times 0.8388 + 2 \times 0.1612$) for the M2. Therefore, it is assumed that the cavity C2 is more negative in electronic state than the C1. Namely, the cavity C2 seems to be more suitable for the location of the K ion than the C1, which is confirmed by the occupation mode of K ions in the tunnel. The K content per cavity is higher for the cavity C2 than the C1 as mentioned in the following part.

3.2. K ions in the tunnel

Joint probability density function (Joint-pdf) [18] for K ions is shown in Fig. 4. The K1 is practically at the center of the cavity C1. K3 and K5 ions are also accommodated in the cavity C1, although the positions of these ions significantly deviate from the cavity center. On the other hand, the K2 is at the center of the cavity C2, and two K4 ions are also seen in this cavity. The sum of K contents in the cavity C1 (i.e. $Occ[K1] + Occ[K3] + Occ[K5] = 0.82(4)$) is less than the unity. This is consistent with the fact that some of the K ions are found at positions (K3 and K4) significantly displaced from the center of the cavities. When a cavity C1 is vacant, the K ion in the neighboring C1 cavity shifts toward the vacancy so as to reduce the repulsive interaction between a K ion at the opposite side, which correspond to the K3 ion as schematically shown in Fig. 5a. Also, the K ion in the cavity C2 neighboring to the vacancy shifts and is assigned as the K4. Similarly, when a cavity C2 is vacant, the K ions in the neighboring C1 cavities shift to be assigned as the K5 ions as illustrated in

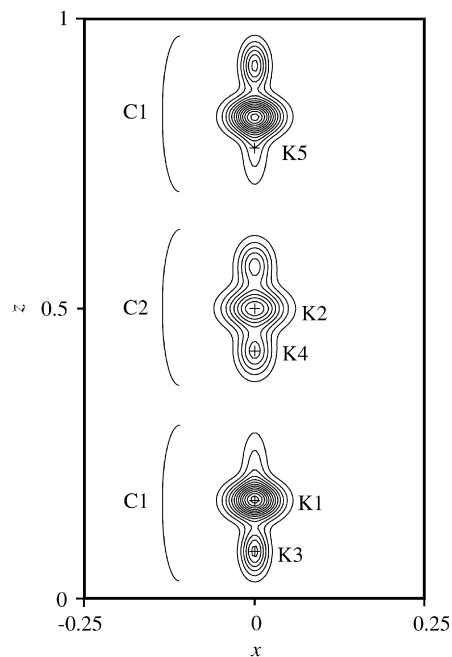


Fig. 4. Joint-pdf for K ions. Contour intervals are $0.25 \text{ atom}/\text{\AA}^3$. K1–K5 sites are indicated by crosses.

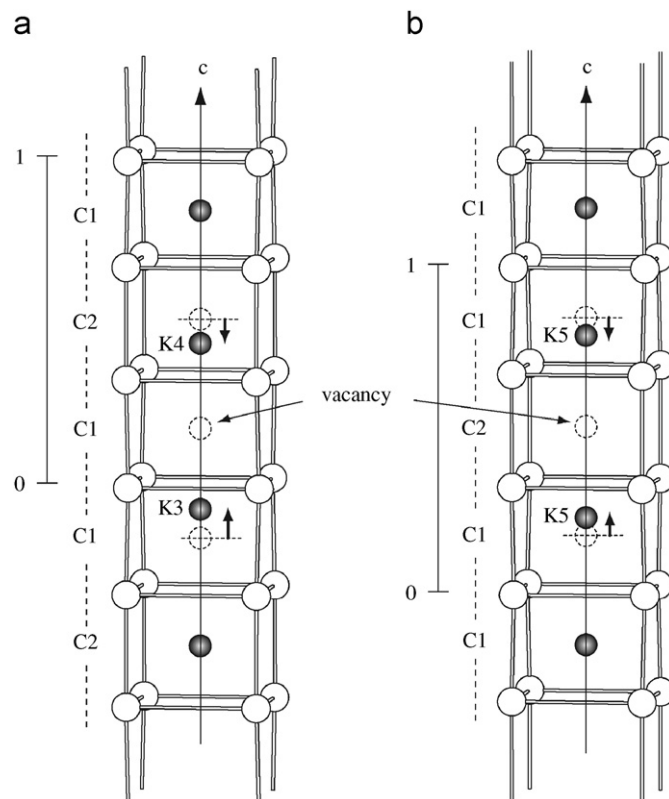


Fig. 5. Schematic representations for the displacement of K ions neighboring to a vacant cavity.

Fig. 5b. Therefore, the observation of the K5 ions requires the partial occupation for the cavity C1, although the sum of K contents for the cavity C2 (i.e. $Occ[K2] + 2Occ[K4]$) is

1.00(5). Considering the estimated error, several percents of C1 cavities seem to be vacant. It is noted that significant residual density of $2.74 \text{ (e/\text{Å}^3)}$ at the K5 position was observed in a difference-Fourier map drawn for a structure model containing no K5 ions.

An average K content per cavity is 0.88 [$= (1.00 + 2 \times 0.82)/3$], which corresponds to the composition parameter $x \approx 1.76$ in a chemical formula $\text{K}_x\text{Mg}_{(8+x)/3}\text{Sb}_{(16-x)/3}\text{O}_{16}$. It is expected that the K concentration in single crystals of hollandite depends on the size of the unit cell. The composition parameter x in chemical formula of Ti-based hollandite $\text{K}_x(\text{M}, \text{Ti})_8\text{O}_{16}$ (M : trivalent or divalent metal) is generally ranging from 1.50 to 1.54 [16,19], while that of Sn-based $\text{K}_x\text{Ga}_x\text{Sn}_{8-x}\text{O}_{16}$ is given by $x \approx 1.88$ [20]. The latter has the larger unit cell ($a = b = 10.389$, $c = 3.132 \text{ \AA}$) than the former (e.g., $a = b = 10.150$, $c = 2.972 \text{ \AA}$ in $\text{K}_{1.54}\text{Mg}_{0.77}\text{Ti}_{7.23}\text{O}_{16}$ [16]), which can be the primary reason of the higher K concentration in the latter. The chemical composition of $x \approx 1.76$ for $\text{K}_x\text{Mg}_{(8+x)/3}\text{Sb}_{(16-x)/3}\text{O}_{16}$ with a subcell of $a = b = 10.3256$, $c_{\text{sub}} = 3.0842 \text{ \AA}$ is supported by the roughly linear correlation between the composition parameter x and unit cell dimensions, especially for the c -axis, in K-hollandite single crystals as shown in Fig. 6. (This is not being the case for those prepared under extreme conditions such as high pressure.) On the other hand, the lattice parameters of $\text{K}_{1.33}\text{Mg}_{3.11}\text{Sb}_{4.89}\text{O}_{16}$ reported by Pring et al. [14] deviate far from this relation as indicated in the figures.

3.3. Ordering scheme

In composite crystals chemical compositions should be related to the ratio of cell dimensions in basic structures for two substructures. Hollandite compounds are generally considered as composite crystals, and the relation for the present hollandite is $c_{\text{h}}/c_{\text{g}} = x/2$, where x is the parameter in a general formula $\text{K}_x\text{Mg}_{(8+x)/3}\text{Sb}_{(16-x)/3}\text{O}_{16}$, and c_{h} and c_{g} are cell dimensions for the basic structure of the host structure and the guest ions, respectively. However, such a relation cannot be found in the present case of $x \approx 1.76$ by any choices of a basic cell for the guest ions so far as the diffraction patterns have 3-fold commensurate character. Beyeler and Schuler [13] obtained single crystals for a phase of $x = \frac{4}{3}$, $\text{K}_{1.33}\text{Mg}_{3.11}\text{Sb}_{4.89}\text{O}_{16}$, and reported diffraction patterns of the superstructure, although no evidence for the chemical composition of the sample was given in the literature. This hollandite, if considered as a composite crystal, satisfies the above relation by taking the basic cell for the substructure of guest ions as $c_{\text{g}}^* = 2c_{\text{h}}^*/3$ (or $c_{\text{h}}/c_{\text{g}} = \frac{2}{3}$). Pring et al. [14] performed the computer simulation for electron diffraction patterns of a polycrystalline sample of the same hollandite, and concluded that the superlattice formation was attributed to the ordering of K ions in tunnels rather than the Mg/Sb ordering in the host structure. They proposed the K arrangement in a tunnel consisting of K–K pairs separated by vacancies; –K–K–·–K–K–·–K–K–..., where · is a vacancy.

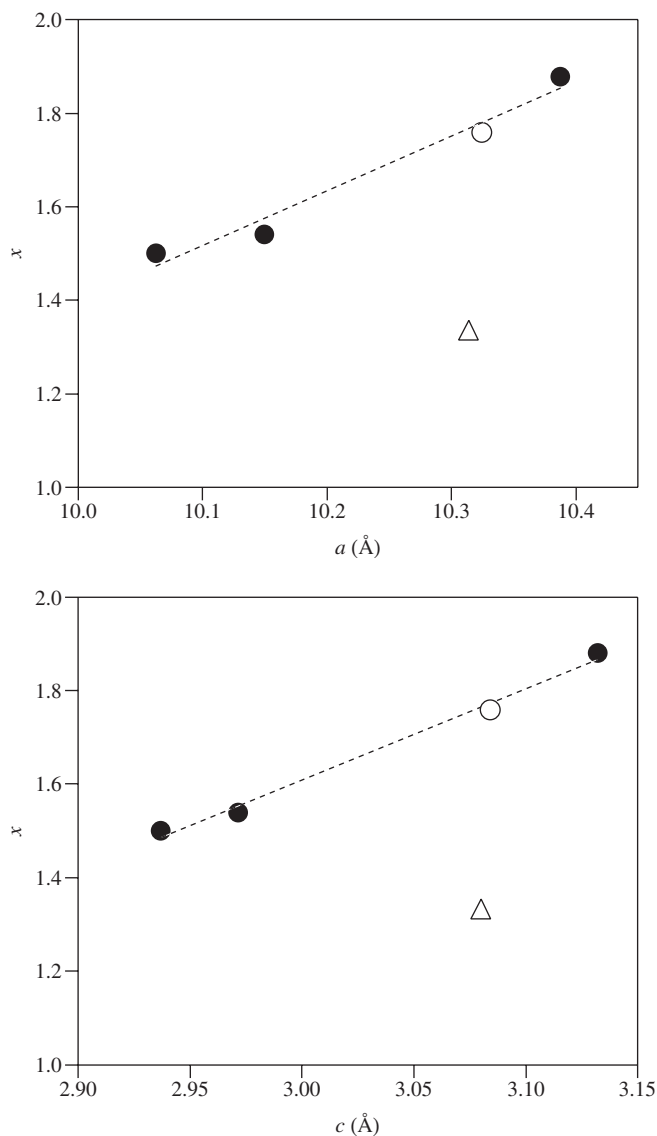


Fig. 6. K ion concentration plotted against the cell dimension in hollandite structures. Filled circles are $\text{K}_{1.54}\text{Mg}_{0.77}\text{Ti}_{7.23}\text{O}_{16}$ [16], $\text{K}_{1.50}\text{Al}_{1.50}\text{Ti}_{6.50}\text{O}_{16}$ [19], and $\text{K}_{1.88}\text{Ga}_{1.88}\text{Sn}_{6.12}\text{O}_{16}$ [20]. Open circles are $\text{K}_{1.76}\text{Mg}_{3.25}\text{Sb}_{4.75}\text{O}_{16}$ (this work), and triangles are $\text{K}_{4/3}\text{Mg}_{28/9}\text{Sb}_{44/9}\text{O}_{16}$ [14]. Subcells are used for c -axis of $\text{K}_x\text{Mg}_{(8+x)/3}\text{Sb}_{(16-x)/3}\text{O}_{16}$.

On the other hand, the structure refinement in the present study for a phase of $x = 1.76$ has revealed that the formation of the 3-fold superstructure is primarily attributed to the occupational modulation of metal ions in the host structure. This is similar to the phenomenon seen in trirutile MgSb_2O_6 . Occupation modes of the K ion (i.e., total K content and joint-pdf) in two cavities, C1 and C2, are a little different, which seems to have arisen from the Mg/Sb modulation. Thus, the ordering scheme in this hollandite is different from those of usual hollandite structures, in which the ordering of guest ions are responsible for observation of commensurate or incommensurate satellite reflections.

The model by Pring et al. is simple and directly related to the chemical composition of $x = \frac{4}{3}$ as seen for composite

crystals. Therefore, it is of interest to unambiguously determine the ordering scheme of the phase $x = \frac{4}{3}$ by X-ray diffraction experiments. According to Bayer and Schuler [13], single crystals of $K_{1.33}Mg_{3.11}Sb_{4.89}O_{16}$ hollandite were grown by heating a stoichiometric oxide mixture in a sealed Pt tube at 1500 °C, followed by the slow cooling at a rate of -10 °C/h. Polycrystalline samples analyzed by Pring et al. were prepared by the slow cooling (-10 °C/h) for a mixture of the same composition from 1250 °C to room temperature [14]. However, as far as I tried, the products from similar syntheses contained trirutile ($MgSb_2O_6$) and/or ilmenite ($Mg_4Sb_2O_9$) along with hollandite. Coexistence of the trirutile and/or ilmenite phases implies that obtained hollandite phases have the higher K concentration than that of the starting mixture of $x = \frac{4}{3}$. Thus, no single crystal or polycrystalline sample of $K_{1.33}Mg_{3.11}Sb_{4.89}O_{16}$ was obtained in my experiments.

Acknowledgement

The author is grateful to Mr. Kosuke Kosuda at NIMS for performing EPMA.

Appendix A. Supplementary Materials

Supplementary data associated with this article can be found in the online version at [doi:10.1016/j.jssc.2007.04.006](https://doi.org/10.1016/j.jssc.2007.04.006).

References

- [1] A.E. Ringwood, S.E. Kesson, N.G. Ware, W. Hibberson, A. Major, *Nature* 278 (1979) 219–223.
- [2] S.K. Khanna, G. Gruner, R. Orbach, H.U. Beyeler, *Phys. Rev. Lett.* 47 (1981) 255–257.
- [3] S. Yoshikado, T. Ohachi, I. Taniguchi, Y. Onoda, M. Watanabe, Y. Fujiki, *Solid State Ionics* 7 (1982) 335–344.
- [4] H.U. Beyeler, *Phys. Rev. Lett.* 37 (1976) 1557–1560.
- [5] T. Ishii, *Solid State Ionics* 9/10 (1983) 1333–1336.
- [6] L.A. Brussaard, H. Boysen, A. Fasolino, T. Janssen, *Acta Crystallogr. A* 58 (2002) 138–145.
- [7] Y. Michiue, M. Watanabe, *Phys. Rev. B* 59 (1999) 11298–11302.
- [8] F.C. Mijlhoff, D.J.W. Ijdo, H.W. Zandbergen, *Acta Crystallogr. B* 41 (1985) 98–101.
- [9] A. Fanchon, J. Vicat, J.-L. Hodeau, P. Wolfers, D.T. Qui, P. Strobel, *Acta Crystallogr. B* 43 (1987) 440–448.
- [10] R.W. Cheary, R. Squadrito, *Acta Crystallogr. A* 48 (1992) 15–27.
- [11] M.L. Carter, R.L. Withers, *J. Solid State Chem.* 178 (2005) 1903–1914.
- [12] H. Leligny, Ph. Labbe, M. Ledesert, B. Raveau, C. Valdez, W.H. McCarroll, *Acta Crystallogr. B* 48 (1992) 134–144.
- [13] H. Beyeler, C. Schuler, *Solid State Ionics* 1 (1980) 77–86.
- [14] A. Pring, D.J. Smith, D.A. Jefferson, *J. Solid State Chem.* 46 (1983) 373–381.
- [15] H.-P. Weber, H. Schulz, *Solid State Ionics* 9/10 (1983) 1337–1340.
- [16] V. Petricek, M. Dusek, L. Palatinus, *The Crystallographic Computing System JANA2000*. Institute of Physics, Praha, Czech Republic, 2000.
- [17] R.D. Shannon, *Acta Crystallogr. A* 32 (1976) 751–767.
- [18] R. Bachmann, H. Schulz, *Acta Crystallogr. A* 40 (1984) 668–675.
- [19] M. Watanabe, Y. Fujiki, Y. Kanazawa, K. Tsukimura, *J. Solid State Chem.* 66 (1987) 56–63.
- [20] K. Fujimoto, S. Ito, M. Watanabe, *Solid State Ionics* 177 (2006) 1901–1904.